

## Mössbauer study of $\text{FeNH}_4(\text{SO}_4)_2 \cdot 12\text{H}_2\text{O}$ at temperatures below $1^\circ\text{K}$

J. L. Groves, A. J. Becker, L. M. Chirovsky, G. W. Wang, and C. S. Wu

*Department of Physics, Columbia University, New York, New York 10027*

(Received 8 May 1978)

A Mössbauer spectrometer mounted in a  $^3\text{He}$ - $^4\text{He}$  dilution refrigerator has been used to study the magnetic properties of hydrated ferric ammonium sulfate [ $\text{FeNH}_4(\text{SO}_4)_2 \cdot 12\text{H}_2\text{O}$ ] from  $4.2^\circ\text{K}$  down to  $0.012^\circ\text{K}$  in zero or small externally applied magnetic fields ( $H_{\text{applied}} < 3.0 \text{ kG}$ ). The zero-field Mössbauer spectra show that hydrated ferric ammonium sulfate undergoes a magnetic transition in the region  $0.024$ – $0.029^\circ\text{K}$ . The spectra taken in an applied field show relaxation effects that are both field and temperature dependent. A stochastic relaxation model was used in the analysis of the Mössbauer data.

### I. INTRODUCTION

Hydrated ferric ammonium sulfate [ $\text{FeNH}_4(\text{SO}_4)_2 \cdot 12\text{H}_2\text{O}$ ] is one of a large number of compounds that have magnetic ordering temperatures below  $1^\circ\text{K}$ . These materials are particularly interesting since the weak cooperative behavior may be the result of exchange, superexchange, or long-range dipole interactions. Owing to the difficulty of cooling samples below  $1^\circ\text{K}$  and maintaining constant temperatures for appreciable times, few materials have been studied at these ultralow temperatures. However, the recent development of the  $^3\text{He}$ - $^4\text{He}$  dilution refrigerator which can provide continuous cooling at any selected temperature down to about  $0.010^\circ\text{K}$  and maintain that temperature to within 1% or better for weeks has made a wide variety of experimental techniques practical; in particular, precision Mössbauer-effect measurements can now be undertaken at these ultralow temperatures. The Mössbauer effect is a powerful tool for studying the magnetic behavior and relaxation effects in many of these weakly coupled magnetic compounds.

Hydrated ferric ammonium sulfate (FAS) is a high-spin ferric compound that has been studied in detail in the temperature range ( $1$ – $300^\circ\text{K}$ ).<sup>1–22</sup> The Mössbauer spectra of FAS in zero or small externally applied fields ( $H < 3.0 \text{ kG}$ ) show relaxation broadening over the entire temperature range previously studied ( $1$ – $300^\circ\text{K}$ ).<sup>11–22</sup> Since specific-heat measurements indicate that FAS has an ordering temperature of about  $0.026^\circ\text{K}$ ,<sup>3</sup> we decided to extend the Mössbauer measurements from  $1^\circ\text{K}$  down to  $0.012^\circ\text{K}$  studying both the magnetic ordering and the relaxation effects as a function of temperature.

### II. EXPERIMENTAL PROCEDURE

A Mössbauer spectrometer mounted in a  $^3\text{He}$ - $^4\text{He}$  dilution refrigerator was used for our Möss-

bauer study of FAS at temperatures below  $1^\circ\text{K}$ .

The dilution refrigerator was obtained from the SHE Corp. and was modified for low-energy Mössbauer spectroscopy work by providing central access to the mixing chamber and Mylar windows between the source and detector. An Elscint MVT-3 Mössbauer driver was mounted on top of the refrigerator with a drive rod extending down to the mixing chamber. The Mössbauer source was  $10 \text{ mCi}$  of  $^{57}\text{Co}$  in Cu and was shielded to minimize the radiation absorbed by the mixing chamber. The radiation shield and the  $^{57}\text{Co}$  source were thermally anchored to the  $1^\circ\text{K}$  jacket around the refrigerator. The temperature of the  $^{57}\text{Co}$  source was approximately  $1.5^\circ\text{K}$ .

The preparation and handling of the FAS absorber required special care since FAS loses water in dry air or a vacuum and undergoes a chemical change. Consequently, the absorber was prepared from crystals of FAS grown from a saturated solution and crushed in a glove bag containing air saturated with water vapor. A special absorber holder was designed which made use of differential contraction so that it sealed at room temperature during the assembly and pump down and broke open spontaneously upon cooling in order for the FAS to have good thermal contact with the liquid helium in the mixing chamber. After the experiment the FAS absorber was examined and found to have its original color, indicating that its water of hydration were still present.

The absorber holder was placed in the mixing chamber as shown in Fig. 1. The temperature of the liquid  $^3\text{He}$ - $^4\text{He}$  mixture surrounding the FAS absorber was controlled by the dilution refrigerator, and measured by a small CMN (cerium magnesium nitrate) thermometer coupled to a SQUID (superconducting quantum-interference device) probe. The temperature was stable to better than 1% for all the runs. At temperatures below  $0.020^\circ\text{K}$ , the Mössbauer spectrum was

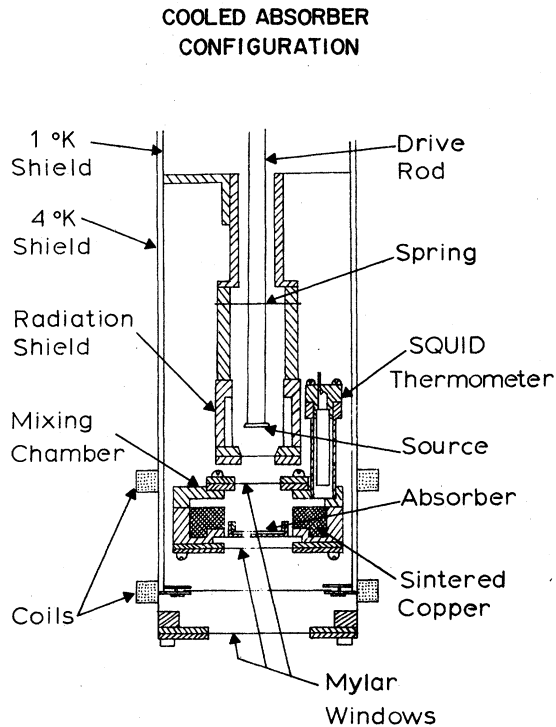


FIG. 1. Experimental configuration for "cooled absorber" studies with the  $^3\text{He}$ - $^4\text{He}$  dilution refrigerator.

used as a thermometer to measure the temperature of the FAS directly.<sup>23</sup> The temperatures of the  $^3\text{He}$ - $^4\text{He}$  mixture and the FAS sample were in agreement to an accuracy of  $0.001^\circ\text{K}$  at the lowest temperature studied. Since the temperature gradient between the FAS sample and the helium mixture decreases with increasing temperature, the CMN thermometer gave an accurate reading of the absorber temperature over the entire range.

Some of the Mössbauer spectra of FAS were taken in externally applied magnetic fields parallel to the direction of observation. These small fields ( $H_{\text{app}} < 3.0$  kG) were produced by a set of superconducting Helmholtz coils mounted on the  $4.2$ - $^\circ\text{K}$  vacuum can for the refrigerator which was immersed in the liquid-helium bath. The magnetic field at the Mössbauer source was less than  $1$  kG for the highest field used.

The Mössbauer spectrometer was operated in the symmetric constant-acceleration mode. The triangular reference wave form was generated by integrating a square wave obtained from the address scaler of a multichannel analyzer operating in the time mode. The frequency of the reference signal was carefully adjusted for optimum performance of the spectrometer (the optimal frequency was approximately  $5$  cps). A  $0.0063$ -mm iron foil absorber was used for calibrating the

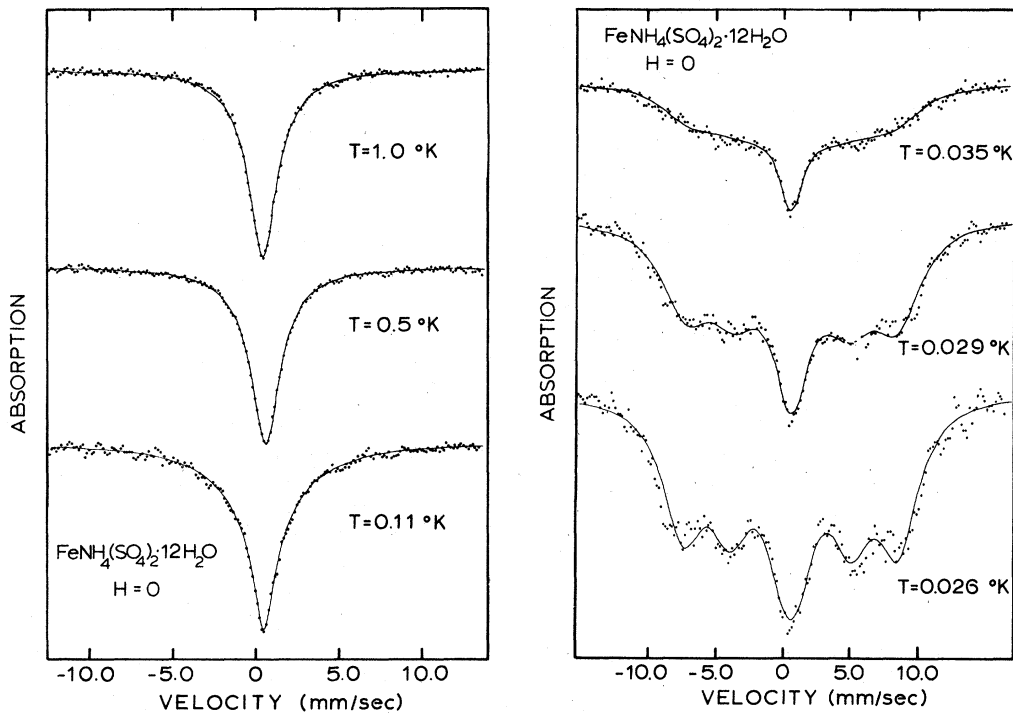


FIG. 2. Mössbauer spectra of FAS at zero applied field above  $25$  mK.

spectrometer and the average linewidth observed for the two inner lines was 0.24 mm/sec. The data were analyzed using one of the models described in Sec. III. A detailed description of the experimental apparatus will be given in a subsequent paper.

### III. EXPERIMENTAL RESULTS

Mössbauer spectra were obtained for FAS with absorber temperatures from 4.2°K down to 0.012°K in zero or small externally applied magnetic fields ( $H_{\text{app}} < 3.0$  kG). The spectra taken in zero applied field at temperatures greater than 0.1°K contain a single very broad line that is approximately Lorentzian with a linewidth of about 2.0 mm/sec. As the temperature is decreased below 0.1°K the Mössbauer spectrum

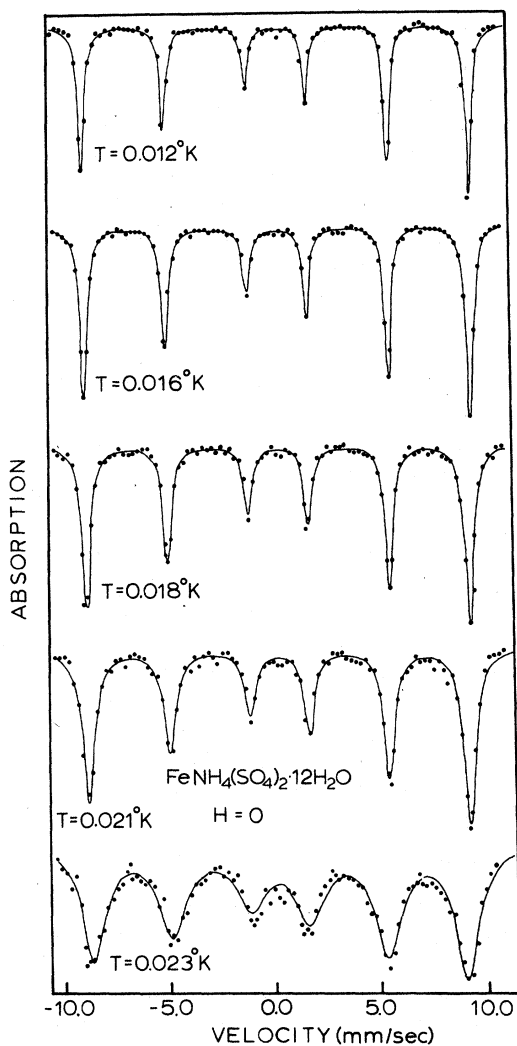


FIG. 3. Mössbauer spectra of FAS below the magnetic transition temperature.

broadens and shows an increasing amount of structure until at about 0.020°K the full six-line nuclear Zeeman pattern is well resolved (see Fig. 2). Below 0.020°K the nuclear Zeeman pattern sharpens and the splitting increases as the temperature decreases as shown in Fig. 3. The zero-field Mössbauer spectra clearly show that FAS undergoes a magnetic transition in the region 0.024–0.029°K in agreement with  $T_{\text{Net}} = 0.026$ °K found from specific-heat measurements.<sup>3</sup> The spectra taken in an applied field showed relaxation effects that are both field and temperature dependent as shown in Fig. 4.

Only the Mössbauer spectra obtained below 0.020°K in zero applied fields can be analyzed without considering relaxation effects. Consequently, the FAS Mössbauer spectra will be discussed in two parts. First, the data obtained below 0.020°K will be analyzed in the effective-field approximation using a conventional Lorentzian least-squares fitting procedure. Then, the relaxation effects in FAS will be discussed and some of the spectra analyzed using a stochastic relaxation model.

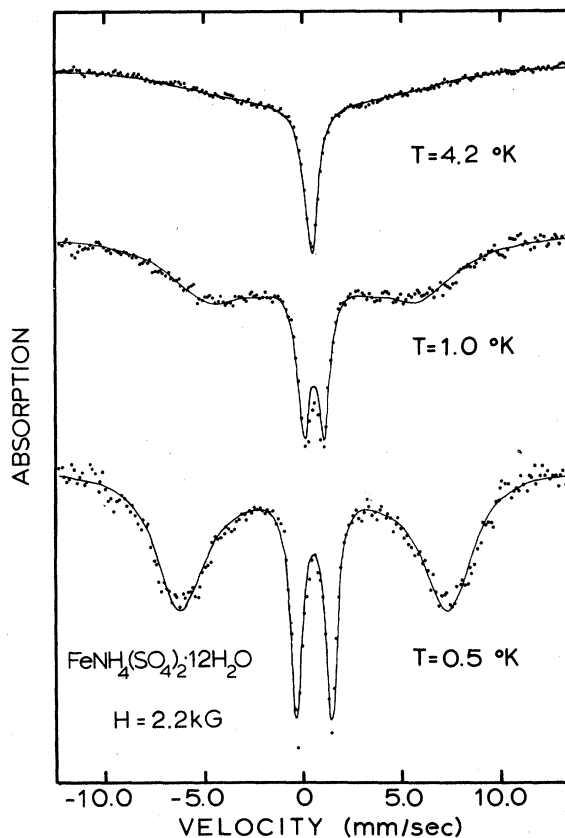


FIG. 4. Mössbauer spectra of FAS in a parallel applied field of 2.2 kG.

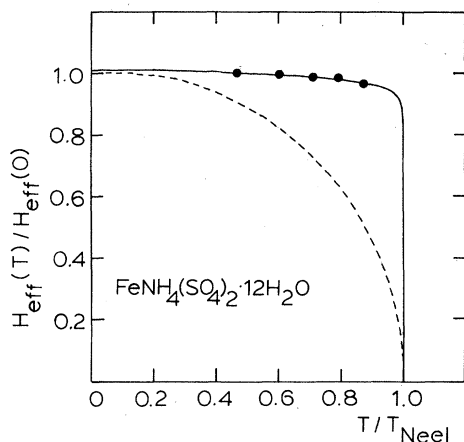


FIG. 5. Temperature dependence of the effective hyperfine field for FAS in the ordered state.

#### IV. EFFECTIVE HYPERFINE FIELD IN THE ANTI-FERROMAGNETIC STATE

The spectra obtained in zero applied field at temperatures below  $T_{\text{Néel}}$  have been analyzed treating the spectra as having arisen from a nuclear Zeeman effect. The effective magnetic field can be determined from the positions of the peaks. The quadrupole interaction is consistent with zero. The parameters adjusted in a least-squares analysis were the hyperfine field, the isomer shift, the linewidths, the line intensities and the background. Figure 3 shows some typical spectra with their corresponding fits for this region. Figure 5 shows the derived temperature dependence of the effective hyperfine field below the Néel temperature.

The internal magnetic field in a magnetically ordered material at any given site is generally proportional to the magnetization at that site.<sup>24</sup> Since in the molecular-field approximation, the temperature dependence of the magnetization follows a Brillouin function, the temperature dependence of the effective field from Mössbauer studies is frequently described by a Brillouin function. Consequently, the  $S = \frac{5}{2}$  Brillouin function is also shown in Fig. 5 for comparison with the data. As can be clearly seen, the Brillouin function cannot represent the temperature dependence. This is not very surprising for a number of reasons: (i) The molecular-field approximation may not be valid in this case. (ii) The effective magnetic fields measured from the Mössbauer spectra depend upon the relaxation mechanism. (iii) The crystal-field splitting of the  $S = \frac{5}{2}$  ground state is of the same order as the interaction responsible for the magnetic ordering.

In magnetically ordered systems the tempera-

ture dependence of the sublattice magnetization  $M(T)$  just below the critical temperature ( $T_N$ ) can usually be described by a power law. That is,

$$\frac{M(T)}{M(0)} = \frac{H(T)}{H(0)} = B \left(1 - \frac{T}{T_N}\right)^\beta, \quad (1)$$

where  $\beta$  and  $BH(0)$  are adjustable parameters. Recently, Mössbauer measurements on high-spin antiferromagnetic ferric compounds  $\text{FeCl}_3$  and  $\text{FeBr}_3$  have shown that the effective hyperfine field follows the above power law for nearly all temperatures less than  $T_N$ .<sup>25,26</sup> We have also used the above equation to fit our data, and the result is shown in Fig. 5. During the fitting process  $T_N$  was fixed at  $0.026^\circ\text{K}$  and  $BH(0)$  and  $\beta$  were variable parameters. The resulting fit is quite satisfactory. Since the effective field is almost independent of temperature up to  $0.8 T_N$ , a rather small value of  $\beta$  is obtained. We find  $\beta = 0.024$  and  $BH(0) = 580 \text{ kG}$ .

#### V. RELAXATION EFFECTS IN FAS

All the Mössbauer spectra of FAS obtained at temperatures from about  $0.020$  to  $1.0^\circ\text{K}$  show pronounced relaxation effects and a simple analysis using Lorentzian least-squares fitting techniques would not be adequate. Previous workers studying FAS at temperatures of  $1^\circ\text{K}$  or above analyzed their results using a variety of relaxation models.<sup>11-22</sup> The most successful and generally applicable relaxation calculations were based on a stochastic model introduced by Kubo<sup>27</sup> and Anderson<sup>28</sup> and later generalized by Blume, Tjon, and Clauser.<sup>29-32</sup> These stochastic models can be numerically solved for all relaxation times, and in many cases a theoretical Mössbauer spectrum can be calculated sufficiently fast that least-squares fitting the theoretical spectrum to data is practical. Consequently, we will analyze and discuss our spectra in the framework of stochastic relaxation theories.

In stochastic models for the Mössbauer line shape, the Hamiltonian describing the electron-nuclear system is written as the sum of time-independent  $H_0$  and time-dependent  $H(t)$  parts:

$$H = H_0 + H(t). \quad (2)$$

The time-independent Hamiltonian  $H_0$  gives the stationary states of the system.  $H(t)$  represents those time-dependent interactions that cause transitions between the stationary states of the nuclear-electron system. In the stochastic relaxation models the transitions are assumed to occur instantaneously and randomly. However, the probability of a transition from any stationary

state to every other stationary state must be specified.

In general, the stationary part can be written

$$H_0 = H_n + H_{ne} + H_e, \quad (3)$$

where  $H_n$  and  $H_e$  contain only nuclear and electronic operators, respectively, and  $H_{ne}$  contains those terms made up of products of nuclear and electronic operators. Many different cases can be described depending on the terms in  $H_0$  and their relative magnitudes.

Consequently, before relaxation spectra can be simulated, a set of stationary states of the electron-nuclear system for the ferric ions in FAS must be obtained. The electronic ground state of a free ferric ion is  ${}^6S_{5/2}$ . In crystalline FAS other  $J = \frac{5}{2}$  states are mixed into the ground  ${}^6S_{5/2}$  sextet by the spin-orbit interaction and, as a consequence, the crystalline electric field can lift some of the degeneracy of the  ${}^6S_{5/2}$  state. If the symmetry of the electric field is cubic, the  ${}^6S_{5/2}$  state splits into a quartet and a doublet; with lower symmetry the  ${}^6S_{5/2}$  state splits into three Kramers doublets. The symmetry of the crystalline field at the ferric ions has not been unambiguously established. At room-temperature x-ray diffraction studies show that each ferric ion is surrounded by an almost regular octahedron of water molecules which may be elongated along one  $\text{H}_2\text{O}-\text{Fe}-\text{H}_2\text{O}$  axis.<sup>33</sup> The analysis of specific heat, magnetic susceptibility, and electron-spin-resonance data<sup>6-10</sup> indicates that the overall splitting of the  ${}^6S_{5/2}$  state is about  $0.1 \text{ cm}^{-1}$  but there is little agreement on the size of the noncubic term in  $H_{\text{CEF}}$ . Consequently, we write  $H_{\text{CEF}}$  for the  ${}^6S_{5/2}$  state in its most general form. Choosing the  $z$  axis along a cube diagonal, the crystal-field potential is assumed to be

$$H_{\text{CEF}} = A_4 [Y_4^0 + (\sqrt{10}/\sqrt{7})(Y_4^{-3} - Y_4^3)] + A_2 Y_2^0. \quad (4)$$

The coefficients  $A_4$  and  $A_2$  are treated as parameters whose values are to be determined from the experimental data.

If magnetic fields are present at the ferric ions in FAS, then the Zeeman interaction must also be included when determining the electronic state of the ferric ions. In this model for FAS only the externally applied magnetic fields will be included in  $H_0$ . The interaction of the ferric ions in FAS with other neighboring magnetic ions will be included in  $H(t)$  since at the very low temperatures used in this study, the relaxation effects are the result of spin-spin interactions. Also, the nuclear and electronic systems can be treated separately since  $H_{ne}$  is of the order of  $0.006^\circ\text{K}$ , whereas  $H_{\text{CEF}}$  and  $H_{\text{Zeeman}}$  yield splitting of the or-

der of  $0.1-1^\circ\text{K}$  or larger. In an applied field the electronic states depend on the magnitude and orientation of the magnetic field relative to the crystalline axes. Considerable simplification occurs if  $H_{\text{CEF}} \gg H_{\text{Zeeman}}$  (zero or small-field case) or if  $H_{\text{Zeeman}} \gg H_{\text{CEF}}$  (high-field case). The stochastic theory of Mössbauer relaxation is easiest to apply to the high-field case; consequently, these spectra will be discussed first. A 2-kG applied field will give an overall splitting for the ferric  ${}^6S$  state of  $0.3^\circ\text{K}$  and since this splitting is considerably larger than the splitting due to  $H_{\text{CEF}}$ , all spectra taken in 2-kG external fields or larger will be analyzed in the high-field approximation.

In the high-field approximation the  ${}^6S$  state is split by the electronic Zeeman interaction, and  $H_{\text{CEF}}$  is then treated as a first-order perturbation. The resulting electronic states are approximately diagonal in  $S_z$  and the nuclear hyperfine interaction can be written

$$H_{ne} = A \vec{I} \cdot \vec{S} \sim A I_x S_x. \quad (5)$$

The product  $A \langle S_x \rangle / g_N \mu_N$  is an effective hyperfine field at the nucleus whose value depends on which electronic state is occupied. The relaxation effects in the Mössbauer spectra are then a consequence of transitions induced by  $H(t)$  between these states and resulting in a fluctuating hyperfine field along the applied-field direction. In the stochastic model of Blume and Tjon,<sup>29</sup>  $\langle S_x \rangle$  is assumed to be a stochastic variable; that is  $\langle S_x \rangle$  a random function of time and can take on any allowed value.

In this stochastic model for longitudinal relaxation, the Mössbauer line shape is proportional to<sup>29</sup>

$$\begin{aligned} \phi(v) \propto \text{Re} \sum_{\substack{m_0, m_1 \\ a, a'}} | \langle I_0 m_0 | H_a | I_1 m_1 \rangle |^2 p(a) \\ \times \langle a | [ \underline{p}(v) \underline{1} - \underline{w} - i\alpha(m_0, m_1) \underline{F} ]^{-1} | a' \rangle. \end{aligned} \quad (6)$$

In the above equation the matrix element  $\langle I_1 m_1 | H_a | I_0 m_0 \rangle$  represents the Mössbauer absorption of a photon by a nucleus going from initial state  $|I_0 m_0\rangle$  to final state  $|I_1 m_1\rangle$ .  $P(a)$  is the probability that the initial electronic state  $|a\rangle$  is populated. Also,

$$p(v) = -i(v - v_0) + \frac{1}{2}\Gamma, \quad (7)$$

where  $v$  is the velocity of the source relative to the absorber,  $v_0$  is the isomer shift, and  $\Gamma$  is the sum of the source and absorber linewidths. The quantity  $\alpha(m_0, m_1)$  is given by

$$\alpha(m_0, m_1) = A \mu_N (c/E_\gamma)(g_0 m_0 - g_1 m_1), \quad (8)$$

where  $E_\gamma$  is the Mössbauer transition energy,  $g_0$  is the nuclear  $g$  factor of the ground state of the Mössbauer nucleus, and  $g_1$  is the  $g$  factor of the excited state. The quantity  $A$  is defined in Eq. (5).

The matrix  $\mathbf{1}$  is the identity matrix and  $\underline{w}$  is the electronic transition probability matrix. The off-diagonal elements  $\langle a | \underline{w} | a' \rangle$  are the probability per unit time that the electronic system will go from state  $|a\rangle$  to state  $|a'\rangle$ . The matrix  $\underline{w}$  is defined such that  $\sum_{a'} \langle a | \underline{w} | a' \rangle = 0$  with the diagonal elements of  $\underline{w}$  given by

$$\langle a | \underline{w} | a \rangle = - \sum_{a' \neq a} \langle a | \underline{w} | a' \rangle. \quad (9)$$

$\underline{F}$  is a diagonal matrix whose elements are the permissible values of  $\langle S_z \rangle$ ; that is,

$$\langle a | \underline{F} | a' \rangle = \langle a | S_z | a' \rangle \delta_{aa'}. \quad (10)$$

The Mössbauer spectra can be calculated by numerically solving Eqs. (6). However, all the matrix inversions must be carried out at each velocity point. Clauser<sup>32</sup> has shown that the velocity can be removed from the matrix calculations, and that Eq. (6) can then be written

$$\phi(v) \propto \text{Re} \sum_{\substack{m_0, m_1 \\ a, a' \\ \alpha}} \frac{| \langle I_0 m_0 | H_k | I_1 m_1 \rangle |^2 p_\alpha \langle a | B_\alpha(m_0, m_1) \rangle \langle C_\alpha(m_0, m_1) | a' \rangle}{v - v_0 - p_\alpha(m_0, m_1)}, \quad (11)$$

where  $|B_\alpha(m_0, m_1)\rangle$  and  $p_\alpha(m_0, m_1)$  are the eigenvectors and eigenvalues, respectively, of  $-i[\frac{1}{2}\Gamma \mathbf{1} - \underline{w} - i\alpha(m_0, m_1)\underline{F}]$ , and  $\langle C_\alpha(m_0, m_1) |$  are the eigenvectors of the Hermitian conjugate of the above matrix.

The only remaining unknown in Eq. (11) is the form of the electronic transition rate operator  $\underline{w}$ . We assume that the transitions are the result of a spin-spin interaction and that the transitions locally conserve angular momentum. Then, the spin-spin Hamiltonian can be written

$$H_{ss} = \sum_b C_{ab} \vec{S}^a \cdot \vec{S}^b, \quad (12)$$

where  $\vec{S}^a$  is the spin of the Mössbauer ion and  $\vec{S}^b$  is the spin of a neighboring Fe ion. The constants  $C_{ab}$  are made up of dipolar and exchange terms. Using the fact that a neighboring spin is in the state  $|b\rangle$  with probability  $P(b)$  and using the "golden rule" to calculate the transition rate for Mössbauer ions going from  $|a\rangle$  to  $|a'\rangle$ , the off-diagonal matrix elements  $\langle a | \underline{w} | a' \rangle$ , can be written

$$\langle a | \underline{w} | a' \rangle = \pi_0 \sum_{bb'} P(b) | \langle a, b | \vec{S}^a \cdot \vec{S}^b | a', b' \rangle |^2, \quad (13)$$

where

$$\pi_0 \equiv \frac{2\pi}{\hbar} \sum_j (C_{aj})^2 \rho_a. \quad (14)$$

The quantity  $\rho_a$  is the density of states of the electronic levels for the Mössbauer ion. The sum  $b$  and  $b'$  is restricted to energy-conserving transitions. In the analysis of the Mössbauer data,  $\pi_0$  will be treated as an experimental parameter.

$\phi(v)$  as written in Eq. (11) gives the Mössbauer spectrum for a single crystal of FAS in an external field. For a powder absorber an average

over the angles defining the external field direction relative to the crystalline axes must be included since the electronic states  $|a\rangle$  are functions of these angles. The powder average was carried out numerically using a two-dimensional Gaussian quadrature integration program. The CPU (central processor unit) time on an IBM 360-91 for the calculation of a 200-velocity-point Mössbauer spectrum for a powder sample of FAS with 18 integration points was about 10 sec. The spectrum calculating program was incorporated in a least-squares fitting routine, and the parameters available for  $\chi^2$  minimization were the background, an overall intensity, two relative intensities  $v_0, \Gamma, A, \pi_0$ , and the two crystal-field coefficients  $A_2$  and  $A_4$ . During the data analysis, the parameters  $A, A_2$ , and  $A_4$  were constrained to be the same for all spectra. The results of the least-squares analysis are listed in Table I, and examples of the calculated spectra are shown in Fig. 5. The values obtained for  $\pi_0$  are in reasonably good agreement for all the spectra analyzed.

In the zero-applied-field case the crystalline electric field splits the  ${}^6S$  state of the ferric ions in FAS into three Kramers doublets. Choosing the quantization axis to be the axis defined by the crystal-field potential given in Eqs. (4), the three doublets can be written

$$\begin{aligned} \text{upper doublet} &\rightarrow | \pm U \rangle = C_1 | \pm \frac{5}{2} \rangle \pm C_2 | \mp \frac{1}{2} \rangle, \\ \text{middle doublet} &\rightarrow | \pm M \rangle = | \pm \frac{3}{2} \rangle, \\ \text{lower doublet} &\rightarrow | \pm L \rangle = C_2 | \pm \frac{5}{2} \rangle \mp C_1 | \mp \frac{1}{2} \rangle, \end{aligned} \quad (15)$$

where  $C_1$  and  $C_2$  are determined by the coefficients  $A_2$  and  $A_4$  in Eqs. (4). Since some degeneracy remains in the electronic system, the off-diagonal terms due to nuclear hyperfine interactions should

TABLE I. Fitted parameters for high-field FAS spectra.<sup>a</sup>

Absorber temperature (°K)	$\pi_0$ (mm/sec)	Linewidth (mm/sec)	Isomer shift <sup>b</sup> (mm/sec)
4.2	$2.98 \pm 0.23$	$0.44 \pm 0.03$	$0.18 \pm 0.01$
1.0	$2.83 \pm 0.25$	$0.51 \pm 0.04$	$0.17 \pm 0.01$
0.5	$2.12 \pm 0.16$	$0.53 \pm 0.05$	$0.17 \pm 0.02$
0.20	$4.02 \pm 1.66$	$0.73 \pm 0.10$	$0.17 \pm 0.03$
0.053	$2.00 \pm 4.58$	$0.54 \pm 0.04$	$0.17 \pm 0.01$

<sup>a</sup>The above parameters were obtained with  $H_{\text{app}} = 2.2$  kG,  $H_{\text{eff}} = 593$  kG,  $A_2 = -0.012$  cm<sup>-1</sup>, and  $A_4 = 0.016$  cm<sup>-1</sup> where  $A_2$  and  $A_4$  are parameters from the crystal-field Hamiltonian,  $H_{\text{CEF}} = A_4 [Y_4^0 + (\sqrt{10}/\sqrt{7})(Y_4^{-3} - Y_4^3)] + A_2 Y_2^0$ .  $A_4$  and  $A_2$  were determined from Mössbauer spectra of FAS taken in zero applied field. All errors listed are twice the standard deviations obtained from the least-squares fits.

<sup>b</sup>The isomer shifts are given relative to a Fe metal absorber with both source and absorber at room temperature. The second-order Doppler shift correction has not been included. The <sup>57</sup>Co in Cu source was at 1°K for all the above runs.

be considered. However, most of the zero-field spectra were run at temperatures sufficiently low such that only the lowest-lying Kramers doublet was appreciably populated. Since this lowest doublet primarily consists of  $|\pm\frac{5}{2}\rangle$  states, where the off-diagonal terms are not important, the effective-field approximation is also used for the zero-field case. Furthermore, since the transverse components of  $\langle \vec{S} \rangle$  are zero for all the three Kramers doublets, only the longitudinal relaxation is considered. The spectra are then calculated using the model described previously for the high-field case. Here, the electronic states of the systems are given by Eq. (15) and since there is no external field, the average over crystal orientations can be done analytically.

The results of least-squares fitting the stochastic longitudinal relaxation model to the zero-field spectra of FAS are listed in Table II and some sample spectra are shown in Fig. 2. There, the value obtained for  $\pi_0$  is slightly different from that found for the high-field case and the linewidth required for the theoretical spectra is much larger than the linewidth found for the well-resolved FAS spectrum at 0.012°K. The average linewidth of the two innermost lines of FAS at 0.012°K is 0.26 mm/sec. Nevertheless, the relaxed spectra are surprisingly well reproduced by the longitudinal relaxation model.

The broadened linewidths required for the theoretical spectra are the result of the assumptions and approximations made in the relaxation models used. Since no corrections for thickness were included, the linewidths given for the partially collapsed spectra are expected to be greater than

TABLE II. Fitted parameters for zero field FAS spectra.<sup>a</sup>

Absorber temperature (°K)	$\pi_0$ (mm/sec)	Linewidth (mm/sec)	Isomer shift <sup>b</sup> (mm/sec)
4.2	$8.53 \pm 2.90$	$1.45 \pm 0.16$	$0.19 \pm 0.01$
1.0	$11.77 \pm 4.76$	$1.63 \pm 0.15$	$0.20 \pm 0.02$
0.5	$10.05 \pm 2.05$	$1.48 \pm 0.15$	$0.19 \pm 0.01$
0.2	$8.62 \pm 0.92$	$1.32 \pm 0.06$	$0.20 \pm 0.01$
0.11	$7.48 \pm 0.74$	$1.19 \pm 0.07$	$0.21 \pm 0.02$
0.053	$5.97 \pm 0.37$	$1.12 \pm 0.09$	$0.22 \pm 0.03$
0.039	$5.22 \pm 0.22$	$1.31 \pm 0.10$	$0.25 \pm 0.04$
0.035	$4.90 \pm 0.25$	$1.47 \pm 0.17$	$0.21 \pm 0.06$
0.031	$4.61 \pm 0.20$	$1.60 \pm 0.16$	$0.18 \pm 0.06$
0.029	$4.23 \pm 0.63$	$1.75 \pm 0.21$	$0.29 \pm 0.05$
0.027	$3.51 \pm 0.62$	$2.00 \pm 0.22$	$0.25 \pm 0.07$
0.026	$3.65 \pm 0.65$	$1.84 \pm 0.23$	$0.31 \pm 0.07$

<sup>a</sup>The above parameters were obtained with  $H_{\text{eff}} = 593$  kG,  $A_2 = -0.012$  cm<sup>-1</sup>, and  $A_4 = +0.016$  cm<sup>-1</sup>, where  $A_2$  and  $A_4$  are parameters from the crystal-field Hamiltonian,  $H_{\text{CEF}} = A_4 [Y_4^0 + (\sqrt{10}/\sqrt{7})(Y_4^{-3} - Y_4^3)] + A_2 Y_2^0$ .  $A_4$  and  $A_2$  were determined from Mössbauer spectra of FAS taken in zero applied fields. All errors listed are twice the standard deviations obtained from the least-squares fits.

<sup>b</sup>The isomer shifts are given relative to a Fe metal absorber with both source and absorber at room temperature. The second-order Doppler shift correction has not been included. The <sup>57</sup>Co in Cu source was at 1°K for all the above runs.

0.26 mm/sec. The analysis of the high-field spectra using the stochastic longitudinal relaxation model previously described gives quite reasonable linewidths. However, the relaxation model applied to the zero-field spectra gives linewidths that are much larger than expected. This broadening is probably a consequence of the neglected off-diagonal matrix elements in the nuclear hyperfine interaction that have been discussed earlier. The more general and more complex stochastic relaxation models of Clauser and Blume<sup>31</sup> should give narrower linewidths.

Hydrated ferric ammonium sulfate is one of many compounds containing transition-metal ions or rare-earth ions that have magnetic transitions below 1°K. Only a very small fraction of such materials has been studied in the ultralow-temperature region where magnetic transitions occur. These weakly interacting magnetic systems are of particular interest since the magnetic ordering may be the result of superexchange or dipole-dipole interactions rather than the exchange interaction. The Mössbauer effect is a powerful tool for studying many of these compounds that have transition temperatures below 1°K. The Mössbauer spectra obtained as a function of temperature and applied magnetic field contain information about the electronic structure of the Möss-

bauer ion and the magnetic structure of the crystal.

The stochastic theory of relaxation effects in Mössbauer spectra as developed by Blume and co-workers<sup>29-32</sup> has been very useful in the analysis of Mössbauer data. In general, the stochastic model has been found to be in good agreement with the observed spectra for several materials under a variety of experimental conditions. The computer calculation time for a Mössbauer spectrum using a stochastic relaxation theory is often sufficiently short that least-squares fitting the theoretical spectrum to the experimental data is prac-

tical. The combination of ultralow-temperature Mössbauer spectroscopy and data analysis using a stochastic relaxation model will be a powerful probe of weakly interacting magnetic systems.

#### ACKNOWLEDGMENTS

We would like to thank M. Blume for helpful discussions concerning the stochastic model. This work was supported by the National Science Foundation under Grants No. MPS71-03314 and No. NSF PHY76-01524.

- 
- <sup>1</sup>F. E. Obenshain, Louis D. Roberts, C. F. Coleman, D. W. Forester, and J. O. Thomson, *Phys. Rev. Lett.* **14**, 365 (1965).
- <sup>2</sup>F. E. Obenshain, L. D. Roberts, C. F. Coleman, D. W. Forester, and J. O. Thomson, in *Low Temperature Physics LT9* (Plenum, New York, 1965), p. 892.
- <sup>3</sup>O. E. Vilches and J. C. Wheatley, *Phys. Rev.* **148**, 509 (1966).
- <sup>4</sup>T. G. Gleason and J. C. Walker, *Phys. Rev.* **188**, 893 (1969).
- <sup>5</sup>P. A. Montano, H. Schechter, and A. Biran, *Solid State Commun.* **9**, 2029 (1971).
- <sup>6</sup>Paul H. E. Meijer, *Physica* **17**, 899 (1951).
- <sup>7</sup>Shigeru Maekawa, *J. Phys. Soc. Jpn.* **16**, 2337 (1961).
- <sup>8</sup>Shigeru Maekawa, *J. Phys. Soc. Jpn.* **17**, 1208 (1962).
- <sup>9</sup>A. Narasimhamurty, *Indian J. Pure Appl. Phys.* **1**, 140 (1963).
- <sup>10</sup>Izuru Kimura and Norikiyo Uryû, *J. Phys. Soc. Jpn.* **23**, 1204 (1967).
- <sup>11</sup>A. J. F. Boyle and J. R. Gabriel, *Phys. Lett.* **19**, 451 (1965).
- <sup>12</sup>F. van der Wonde and A. J. Dekker, *Solid State Commun.* **3**, 319 (1965).
- <sup>13</sup>J. G. Dash and B. D. Dunlap, *Bull. Am. Phys. Soc.* **11**, 48 (1966).
- <sup>14</sup>Werner Bruckner, Gerhard Ritter, and Horst Wegener, *Z. Phys.* **200**, 421 (1967).
- <sup>15</sup>H. Wegener and G. Ritter, *Z. Angew. Phys.* **24**, 270 (1968).
- <sup>16</sup>B. C. van Zorge, F. van der Wonde, and W. J. Caspers, *Z. Phys.* **221**, 113 (1969).
- <sup>17</sup>H. H. F. Wegener, B. Braunecker, G. Ritter, and D. Seyboth, *Z. Phys.* **262**, 149 (1973).
- <sup>18</sup>L. Campbell and S. DeBenedetti, *Phys. Lett.* **20**, 102 (1966).
- <sup>19</sup>R. M. Housley and H. de Waard, *Phys. Lett.* **21**, 90 (1966).
- <sup>20</sup>R. M. Housley, *J. Appl. Phys.* **38**, 1287 (1967).
- <sup>21</sup>L. E. Campbell and S. DeBenedetti, *Phys. Rev.* **167**, 556 (1968).
- <sup>22</sup>S. Mørup and N. Thrane, *Phys. Rev. B* **4**, 2087 (1971).
- <sup>23</sup>R. D. Taylor, in *Temperature, Its Measurement and Control in Science and Industry*, edited by C. M. Kerzfeld and E. G. Brickwedde, (Reinhold, New York, 1962), Vol. 3, Pt. I, p. 139.
- <sup>24</sup>T. C. Gibb, in *Principles of Mossbauer Spectroscopy* (Wiley, New York, 1976), p. 112.
- <sup>25</sup>J. P. Stampfel, W. T. Oosterhuis, B. Window, and F. de S. Barros, *Phys. Rev. B* **8**, 4371 (1973).
- <sup>26</sup>W. T. Oosterhuis, B. Window, and K. Spartalian, *Phys. Rev. B* **10**, 4616 (1974).
- <sup>27</sup>R. Kubo, *J. Phys. Soc. Jpn.* **9**, 935 (1954).
- <sup>28</sup>P. W. Anderson, *J. Phys. Soc. Jpn.* **9**, 316 (1954).
- <sup>29</sup>M. Blume and J. A. Tjon, *Phys. Rev.* **165**, 446 (1968).
- <sup>30</sup>M. Blume, *Phys. Rev.* **174**, 351 (1968).
- <sup>31</sup>M. J. Clouser and M. Blume, *Phys. Rev. B* **3**, 583 (1971).
- <sup>32</sup>M. J. Clouser, *Phys. Rev. B* **3**, 3748 (1971).
- <sup>33</sup>H. Lipson and C. A. Beevers, *Proc. R. Soc. Lond.* **148**, 664 (1935).